Available online at www.sciencedirect.com
SCIENCE DIRECT®
Journal of Molecular Spectroscopy 221 (2003) 99–105
Journal of MOLECULAR SPECTROSCOPY
www.elsevier.com/locate/jms

Water line parameters for weak lines in the range 9000–12 700 cm^{-1} ☆

Roman N. Tolchenov,[a] Jonathan Tennyson,[a,*] Sergei V. Shirin,[a,1] Nikolai F. Zobov,[a,1] Oleg L. Polyansky,[a,1] and Ahilleas N. Maurellis[b]

[a] *Department of Physics and Astronomy, University College London, London WC1E 6BT, UK*
[b] *SRON National Institute for Space Research, Sorbonnelaan 2, 3584 CA Utrecht, Netherlands*

Received 8 April 2003; in revised form 13 May 2003

Abstract

A total of 7923 transitions previously derived from long pathlength, Fourier transform spectra of pure water vapor (Schermaul et al., J. Mol. Spectrosc. 211 (2002) 169) have been refitted and reanalyzed using a newly calculated variational linelist. Of these, 6600 lines are weaker than 1×10^{-24} cm/molecule, for which reliable intensities are obtained. These weak lines include 1082 lines, largely due to $H_2^{16}O$, which have not been previously observed. A total of 7156 lines were assigned resulting in 329 new energy levels for $H_2^{16}O$ spread over 32 vibrational levels. Estimates are also given for the band origins of the (022), (140), and (051) vibrational states.
© 2003 Elsevier Science (USA). All rights reserved.

Keywords: Water vapor; Line parameters; Atmospheric radiation

1. Introduction

The spectrum of water almost entirely determines the transmission of sunlight through our atmosphere in the near-infrared. It is therefore unsurprising that the spectrum of $H_2^{16}O$ [1–3] as well its isotopomers [4,5] has been measured repeatedly in this region. The cited studies have all provided parameters which are included in the most recent edition of the atmospheric database HITRAN [6].

However the huge dynamic range of the absorption features due to water in the 9000–12 700 cm^{-1} range makes the characterization of the water spectrum very difficult to determine from any single experimental set-up. Different pathlengths are required for differing line strengths in order to avoid saturation (in the case of strong lines) or to ensure sufficient signal (for weak lines). Schermaul et al. [7] recorded a series of long-pathlength Fourier Transform spectra using long integration times. These spectra cover the frequency range 6500–16 500 cm^{-1} in pure water vapor, although the data above 15 400 cm^{-1} are not competitive with that obtained elsewhere [8]. These spectra do not provide useful information on strong water absorption features, which are saturated in this experimental setup, but provide a wealth of information on the weak lines in this spectral region. Schermaul et al.'s spectra divide into three separate portions. The 13 200–15 000 cm^{-1} spectrum [7] and 11 787–13 554 cm^{-1} spectrum [9] have been analyzed previously. In this work we analyze the 9000–12 700 cm^{-1} region (referred to as spectrum 2 hereafter). Recent atmospheric models [10,11] have demonstrated that the addition of weak water absorption lines from the two previously analyzed regions leads to a significant extra absorption of sunlight. It is thus likely that the lines characterized here will have a similar effect.

Of considerable relevance to analysis of newly observed weak lines in this, and other, regions is the calculation of a linelist of water transitions using variational nuclear motion calculations based on a new, spectroscopically determined potential [12]. These new calculations are described below.

☆ Supplementary data for this article are available on ScienceDirect.

* Corresponding author. Fax: +44-20-7679-2564.
E-mail address: j.tennyson@ucl.ac.uk (J. Tennyson).
[1] Permanent address: Institute of Applied Physics, Russian Academy of Science, Uljanov Street 46, Nizhnii Novgorod 603950, Russia.

0022-2852/$ - see front matter © 2003 Elsevier Science (USA). All rights reserved.
doi:10.1016/S0022-2852(03)00171-1

2. Line parameters

In order to retrieve the weak water line parameters in the spectral region 9000–12 700 cm^{-1} spectrum 2 of Schermaul et al. [7] was used. The spectrum was recorded at a temperature 295.7 ± 0.7 K, pressure 22.93 ± 0.08 Pa, and pathlength 800.8 ± 1.0 m. The baseline was corrected by Schermaul et al. [7] and was kept fixed in our fit.

The fit has been performed using interactive spectrum fitting program GOBLIN [13]. The theoretical line shape was assumed to be a generalized Voigt profile in which four parameters (line position, peak height, halfwidth, and damping) are treated as adjustable. The reasons for this choice of parameters are discussed at length by Schermaul et al. [7]. Effects due to saturation were considered in a special way because the region of the spectrum considered here contains many strong lines which are saturated at experimental conditions.

Fits were made to the absorbance, τ, which is also known as the optical depth, defined as the absorption coefficient times the pathlength. First, the parameters of the strong lines were estimated using data from the HITRAN database, then during the fit these parameters were adjusted to find the best possible solution for unsaturated parts of the profiles. In the fit it was assumed that the spectral points with absorbance $\tau \leqslant 0.9$ are not distorted by the effects of saturation. The points above this level were excluded from the fit as they could not be accurately represented with our fit function. This is probably due to instrumental effects. Weak lines were fitted simultaneously with the strong lines in whose wings they occurred. Fig. 1 shows a typical case of how the resulting parameters reproduce the experiment in regions with a high concentration of strong lines. The flat regions in the residuals set to zero correspond to the spectral points excluded from the fit. This restriction, which is due to saturation effects, gives an approximate upper limit in intensity of 1×10^{-24} cm/molecule for the lines with reliable parameters obtained from this fit.

It should be noted that for the very strong lines the residuals still show systematic, antisymmetric features, as is illustrated in Fig. 2. The exact cause of this asymmetry is unclear. Possible causes include errors in the phase correction or the effects of adding different runs. The asymmetric profile may, of course, affect significantly the intensities of certain weak lines. We estimate that the error in the intensity for a line with intensity of 7×10^{-27} cm/molecule may be up to 100% if its center lies on the shoulder of a strong line. In a number of cases, the same effect made it impossible to find a stable solution for weak lines (intensities $< 7 \times 10^{-27}$ cm/molecule) because of the significant distortion of the baseline. This problem mostly affects the region around 10 700 cm^{-1}.

Fits to generalized Voigt parameters were obtained for 7923 lines, 6600 of which are weak ones (with intensities less than 1×10^{-24} cm/molecule). These parameters have been used to calculate the line intensities according to the formula

$$S = \frac{T}{T_0 L_0} \frac{A}{pl}, \tag{1}$$

where L_0 is the Loschmidt number 2.686763×10^{19} cm^{-3}/atm, $T_0 = 273.15$ K, T is the water temperature, p is the pressure, l is the pathlength, and A is the absorbance integrated over the line.

The line intensities obtained in our fits have been compared with those from HITRAN [6] in the spectral region 9650–11 400 cm^{-1}. This region was the subject of a recent study by Brown et al. [3], whose data are now

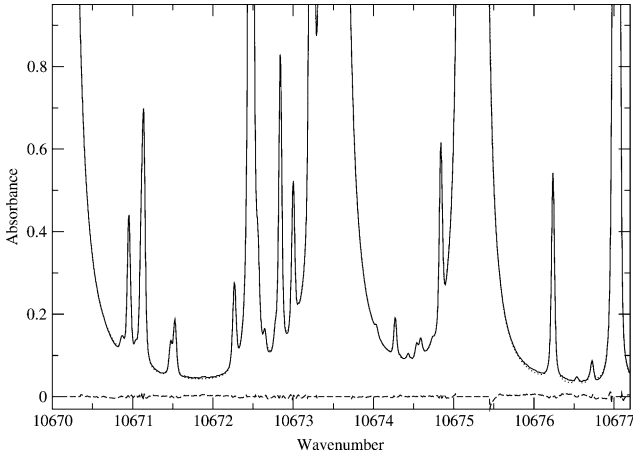

Fig. 1. A portion of the experimental spectrum (solid curve) showing a high density of strong lines. The fitted spectrum (dotted curve) is barely discernible under the experimental spectrum. The dashed curve near the bottom of the plot gives the residual. Regions where the residuals are totally flat and zero were excluded a priori from the fit.

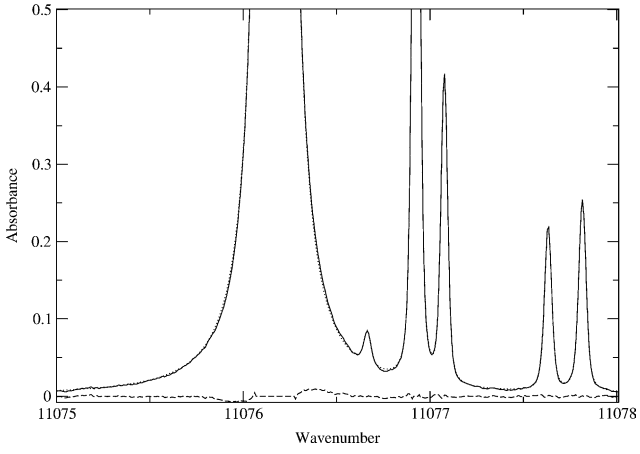

Fig. 2. A typical strong line, $(003)2_{02} - (000)1_{01}$, showing an antisymmetric feature in the residual.

included in HITRAN. Both HITRAN and our dataset contain about 5000 lines in this region, 4000 of which are weak (with intensities smaller than 1×10^{-24} cm/molecule). In order to make the comparison, an automated procedure has been implemented to find line-by-line correspondence between the datasets. The procedure involves searching for the best match both in line position and intensity. If a match could not be found for a line within acceptable intervals of values, it was not included in the comparison. The procedure returned a total number of 2750 matched lines with intensities in the interval (2×10^{-27}–1×10^{-24}) cm/molecule. Approximately 2050 lines of these belong to $H_2^{16}O$, 500 lines to $H_2^{18}O$, and 200 to $H_2^{17}O$. HITRAN actually contains many more $H_2^{18}O$ and $H_2^{17}O$ transitions in this region, but the majority of them are too weak to be seen with the experimental conditions considered here. Our linelist contains 1500 more lines than HITRAN with intensities between 2×10^{-27} and 3×10^{-26} cm/molecule in the 9650–11 400 cm^{-1} spectral region. As shown below, nearly all of these lines correspond to transitions of $H_2^{16}O$.

Fig. 3 gives a comparison for the intensity of line present in both HITRAN and our work. The agreement between the two is satisfactory, with no systematic differences. The larger differences at lower intensities are merely a reflection of the greater error in the line parameters for the weaker lines. Similar agreement is found with the parameters obtained previously for the 11 787–12 700 cm^{-1} region [9] by analyzing another spectrum ("spectrum 3") measured by Schermaul et al. [7].

A full list of 7923 lines fitted in the course of this work is given in the electronic archive. Only the parameters for the 6600 lines weaker than 1×10^{-24} cm/molecule should be considered reliable. Parameters for the stronger lines are determined more reliably from water–air experiments such as those analyzed by Brown et al. [3] or Schermaul et al. [14,15]. For the weaker lines, the list includes statistical uncertainties determined by the fit for each parameter (wavenumber, intensity, self-broadening, damping). In practice we assumed a minimum error of 0.001 cm^{-1} for the transition wavenumber in the analysis below. The damping parameter should represent the ratio of the Lorentzian profile to the total line profile. In practice the parameter was used to obtain good fits to the line profile which are important for accurate intensity determination. This leads to a large spread in values of the damping parameter, especially for weak lines. The values obtained probably have little physical significance. In particular they also help account for the instrument function which was not explicitly allowed for in our fits. Conversely we checked the reliability of our intensities by back modelling. Spectra were synthesized using HITRAN data, convoluted with an approximation to the instrument function and then fitted. The resulting intensities were with 1 % of the initial values.

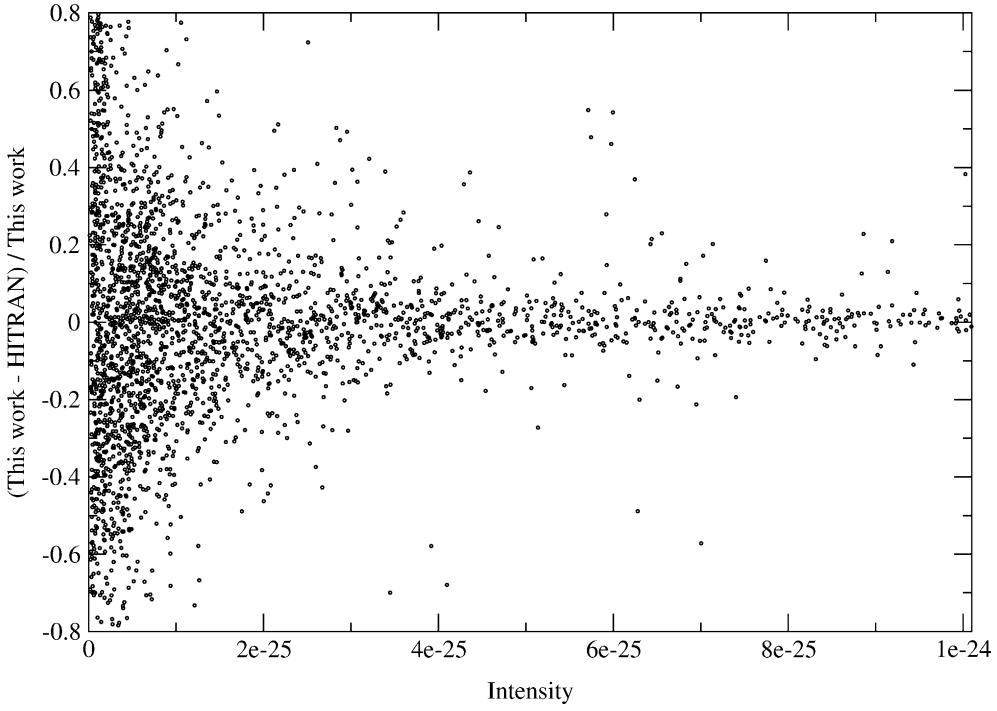

Fig. 3. Relative differences in line intensity for weak water vapor lines obtained from the present work (denoted by "This work") and HITRAN [6] as a function of line intensity from the present work in the range 9000–12 700 cm^{-1}.

3. Line assignment

To aid line assignments a variational water vapor linelist has been calculated using the DVR3D program suite [16] and a new potential surface. This surface, due to Shirin et al. [12], was spectroscopically determined using spectroscopic data for $H_2^{16}O$ up to 25 000 cm^{-1}. Highly converged calculations were performed using Radau coordinates. Thirty-four radial grid points, based on Morse oscillator-like functions [17], were combined with 40 angular grid points based on (associated) Legendre polynomials. In the two-step procedure used [18], a series of Hamiltonians of dimension 2000 were diagonalized for the 'vibrational' first step, the results of which were used to generate Hamiltonians of size $450 \times (J + 1 - p)$ for the second step, where p is the parity. Wavefunctions for all states with $J \leqslant 14$ and energies up to 25 000 cm^{-1} were computed. Energies are usually accurate to within 0.1 cm^{-1}, with somewhat larger errors, up 0.2 cm^{-1}, for states with significant bending excitation. As the energy levels and associated wavefunctions arising from these calculations are only assigned rigorous quantum numbers (J, p, *ortho*/*para*), full assignments were made using the algorithm of Zobov et al. [19], which first assigns the $J = 0$ vibrational states and then uses these to assign the associated rotational levels.

The variational linelist due to Partridge and Schwenke (PS) [20] has been widely used for spectral analysis in the near-infrared and visible. Although our new linelist is not significantly more accurate than PS's in the region considered here, it has a number of advantages. First our assignments proved to be much more reliable and could generally be used unaltered. Second our better convergence of the nuclear motion calculations, particularly for higher Js, removed artifacts due to splitting of quasi-degenerate levels (see [21]). Finally our linelist is reliable in the 15 000–25 000 cm^{-1} region where the PS linelist becomes increasingly erratic. We have previously analyzed a number of water vapor spectra in this region [7,9,22–25]. All these spectra contain a significant number of unassigned lines. We plan to use the new linelist to reanalyze these and other spectra.

Of course many energy levels for $H_2^{16}O$ are known [26], meaning that many transitions could be assigned 'trivially' using known experimental energy differences. After making trivial assignments, our calculated energies were then used to predict spectral regions for searching for combination differences. As a result more than 7156 lines out of 7923 line fitted have been assigned to transitions to 32 upper vibrational states. One thousand and eighty two lines were newly assigned which gave 329 new experimental energy levels. Almost all new assignments are confirmed by combination differences.

The results of the assignment are summarized in Table 1. Our line assignments are given in the electronic archive as are new energy levels for all vibrational states for which more than 10 new levels have been determined. Our new energy levels do not actually contain any direct measurements of previously unknown band origins. However for the (022), (140), and (051) vibrational states, sufficient energy levels with low J have been determined for us to estimate the band origins to within 0.1 cm^{-1}. These estimates are given in Table 1.

Comparison of our assignments with those from HITRAN gave a large number of differences. We could assign about 100 HITRAN's unassigned lines and reassign 84. The remaining disagreements were due to different vibrational labeling and different assignments of blended lines. A list of the re-assigned lines is given in Table 2.

Table 1
Summary of $H_2^{16}O$ transitions newly assigned in the 9000–12 760 cm^{-1} region

Band	ω (cm^{-1})	a	b	Band	ω (cm^{-1})	a	b
130	8273.976	2	2	051	11242.7	34	4
031	8373.850	24	0	131	11813.207	374	4
210	8761.582	14	24	013	12565.007	275	0
111	8806.998	172	6	032	12007.776	146	0
012	9000.136	214	19	112	12407.662	284	4
060	8869.954	9	2	211	12151.255	530	0
022	10521.7	116	162	230	11767.390	155	3
140	9274.2	0	108	310	12139.315	265	7
041	9833.584	280	47	160		5	0
220	10284.367	112	184	061		2	0
121	10328.727	416	94	320		5	0
300	10599.686	398	134	221	13652.656	41	0
201	10613.365	626	75	400	13828.277	5	0
102	10868.876	346	139	301	13830.938	2	0
003	11032.406	417	69	023	14066.194	4	0
150		7	0	202	14221.161	3	0

a denotes trivial assignments, b denotes transitions to newly observed levels.

Table 2
$H_2^{16}O$ lines which are not assigned or incorrectly assigned in HITRAN [6]

HITRAN		This work		New assignment							
Line position (cm^{-1})	Intensity (cm/molecule)	Line position (cm^{-1})	Intensity (cm/molecule)	Upper state				Lower state			
10010.82614	4.340(−26)	10010.82665	2.237(−26)	121	12	1	12	000	13	1	13
10050.87110	5.473(−26)	10050.87003	7.708(−26)	220	9	0	9	000	10	1	10
10078.59953	1.821(−25)	10078.60084	1.914(−25)	041	10	5	5	000	11	3	8
10086.32722	1.414(−25)	10086.32823	1.336(−25)	220	5	5	0	000	6	6	1
10096.03659	5.332(−26)	10096.03504	5.149(−26)	041	6	6	0	000	7	6	1
10119.03051	3.547(−25)	10119.03054	3.574(−25)	150	8	1	8	000	9	0	9
10162.73302	9.296(−26)	10162.73585	8.424(−26)	150	2	1	2	000	3	2	1
10163.00624	4.932(−26)	10163.00690	3.857(−26)	121	10	1	9	000	10	3	8
10169.28618	2.898(−25)	10169.28684	3.014(−25)	041	6	5	1	000	6	5	2
10181.95057	3.764(−25)	10181.95008	3.848(−25)	300	8	3	6	000	9	4	5
10187.89190	1.028(−26)	10187.88622	2.583(−27)	201	13	2	11	000	14	2	12
10194.88590	6.215(−26)	10194.88622	7.585(−26)	201	8	2	6	000	9	4	5
10201.18490	1.636(−26)	10201.18282	6.470(−27)	201	11	5	6	000	12	5	7
10206.14751	8.284(−26)	10206.15294	7.443(−26)	150	1	1	0	000	2	2	1
10207.67671	6.187(−26)	10207.67415	4.776(−26)	220	5	2	4	000	5	3	3
10244.09993	3.695(−26)	10244.09780	1.817(−26)	201	8	8	0	000	9	8	1
10266.95716	2.317(−25)	10266.95628	2.632(−25)	041	7	6	2	000	7	6	1
10267.17113	6.291(−25)	10267.17053	6.049(−25)	041	6	6	0	000	6	6	1
10277.25270	1.832(−25)	10277.25306	2.340(−25)	121	10	4	6	000	11	2	9
10279.70469	6.001(−26)	10279.71150	7.180(−26)	201	6	0	6	000	6	4	3
10313.93830	2.766(−25)	10313.93763	2.765(−25)	220	5	4	1	000	6	3	4
10323.95496	4.231(−26)	10323.95556	8.301(−26)	121	7	7	1	000	8	7	2
10340.09011	4.307(−26)	10340.08814	5.390(−26)	220	4	4	0	000	5	3	3
10345.06216	4.860(−26)	10345.05925	6.441(−26)	022	7	1	7	000	8	0	8
10389.37256	1.495(−25)	10389.37149	9.352(−26)	060	8	6	3	000	8	3	6
10394.72950	1.786(−25)	10394.72438	9.853(−26)	000	0	0	0	000	0	0	0
10412.07428	3.966(−25)	10412.07491	3.402(−25)	000	0	0	0	000	0	0	0
10418.63706	1.084(−25)	10418.63839	1.001(−25)	211	5	1	5	010	6	1	6
10419.47678	4.727(−25)	10419.47925	5.398(−25)	300	8	3	6	000	8	4	5
10432.41368	1.702(−25)	10432.41440	1.554(−25)	201	8	2	6	000	8	4	5
10436.62886	1.700(−25)	10436.62865	1.366(−25)	000	0	0	0	000	0	0	0
10441.35802	1.367(−25)	10441.35693	9.618(−26)	022	3	1	3	000	4	0	4
10441.56480	1.082(−25)	10441.56538	9.258(−26)	000	0	0	0	000	0	0	0
10458.23644	1.657(−25)	10458.23692	1.382(−25)	121	10	3	8	000	11	1	11
10459.61422	5.574(−26)	10459.61120	5.033(−26)	000	0	0	0	000	0	0	0
10463.12214	1.208(−25)	10463.12013	1.348(−25)	022	4	0	4	000	4	1	3
10475.62594	4.465(−26)	10475.62355	2.939(−26)	220	3	3	0	000	3	0	3
10477.95447	3.029(−24)	10477.95539	3.319(−24)	121	10	0	10	000	9	0	9
10494.43602	1.174(−25)	10494.44266	1.052(−25)	220	7	7	1	000	8	6	2
10509.97166	2.547(−25)	10509.97250	2.596(−25)	220	7	5	2	000	7	4	3
10512.50743	4.356(−26)	10512.50583	3.899(−26)	102	9	3	6	000	10	4	7
10553.13104	1.257(−24)	10553.13145	1.210(−24)	060	8	6	3	000	7	3	4
10569.11730	3.617(−25)	10569.11655	3.516(−25)	121	10	3	8	000	9	3	7
10581.24301	9.961(−26)	10581.24203	8.149(−26)	000	0	0	0	000	0	0	0
10598.65118	1.460(−25)	10598.64362	1.184(−25)	022	3	2	2	000	3	1	3
10609.93625	5.436(−26)	10609.93929	7.686(−26)	000	0	0	0	000	0	0	0
10616.79074	6.255(−26)	10616.78581	4.311(−26)	121	6	3	3	000	5	1	4
10619.83240	7.388(−26)	10619.82839	2.286(−26)	000	0	0	0	000	0	0	0
10633.85671	7.513(−26)	10633.86130	7.492(−26)	300	7	7	1	000	7	6	2
10641.87207	2.811(−24)	10641.87143	3.010(−24)	102	3	3	0	000	4	4	1
10660.09980	2.652(−25)	10660.09848	3.522(−25)	003	11	3	8	000	12	3	9
10661.38868	6.126(−26)	10661.39181	1.786(−26)	310	8	1	8	010	7	0	7
10665.99367	4.102(−26)	10665.99680	8.432(−26)	022	9	4	5	000	8	5	4
10685.28759	1.508(−25)	10685.28651	1.431(−25)	220	8	7	2	000	8	6	3
10689.81356	2.700(−25)	10689.81386	3.422(−25)	220	7	7	0	000	7	6	1
10691.27332	4.853(−26)	10691.27578	8.100(−26)	102	8	0	8	000	8	1	7
10698.21747	5.154(−26)	10698.22456	7.699(−26)	003	9	5	5	000	10	5	6
10714.47577	4.977(−26)	10714.48494	2.942(−26)	022	8	5	4	000	8	4	5
10714.92553	3.672(−26)	10714.92271	6.680(−26)	102	7	1	7	000	7	2	6
10726.84334	2.544(−25)	10726.83658	1.981(−25)	022	5	5	0	000	5	4	1

Table 2 (*continued*)

HITRAN		This work		New assignment							
Line position (cm^{-1})	Intensity (cm/molecule)	Line position (cm^{-1})	Intensity (cm/molecule)	Upper state				Lower state			
10753.47800	8.368(−26)	10753.49321	1.307(−25)	201	11	6	5	000	10	6	4
10760.49873	8.235(−26)	10760.49929	8.442(−26)	000	0	0	0	000	0	0	0
10762.65584	7.534(−26)	10762.65655	4.907(−26)	102	6	6	0	000	7	5	3
10774.64154	8.554(−26)	10774.64116	7.060(−26)	022	6	6	1	000	6	5	2
10776.59861	2.200(−24)	10776.59922	1.892(−24)	022	9	3	7	000	8	2	6
10784.23961	6.150(−26)	10784.24283	7.466(−26)	102	6	3	3	000	7	2	6
10865.35760	1.734(−25)	10865.35849	1.330(−25)	102	4	2	3	000	3	3	0
10927.33332	7.167(−25)	10927.33270	7.175(−25)	022	6	5	2	000	6	2	5
11058.80922	3.061(−24)	11058.81371	4.083(−24)	102	5	5	0	000	4	4	1
11082.08505	1.227(−25)	11082.07673	1.151(−25)	003	7	6	2	000	6	6	1
11098.34943	9.941(−25)	11098.34816	1.206(−24)	000	0	0	0	000	0	0	0
11098.40930	9.941(−25)	11098.40699	3.321(−24)	003	6	5	1	000	5	5	0
11126.79413	1.413(−25)	11126.79357	1.462(−25)	000	0	0	0	000	0	0	0
11180.55683	5.791(−25)	11180.55689	5.573(−25)	003	10	2	9	000	9	2	8
11335.14511	4.533(−26)	11335.13333	1.619(−26)	051	3	1	3	000	2	1	2
11386.21206	1.760(−25)	11386.21312	1.795(−25)	003	8	2	6	000	7	0	7

4. Conclusion

Characterizing the near-infrared and visible spectrum of water remains a major research priority because of its importance in atmospheric absorption, and indeed in many other situations. In this work we have fitted and assigned the pure water vapor spectrum of Schermaul et al. [7]. We have shown that this spectrum contains over 1000 more weak water transitions than previous studies of the same region. Most of these transitions are due to $H_2^{16}O$. We have computed a new, accurate variational linelist for studying room temperature water vapor transitions and with its use have assigned more than 90% of lines fitted. This analysis involved relabelling or reassigning about 80 previously analyzed lines as well as assigning about 100 previously observed but unassigned lines. It is to be anticipated that our new linelist will be even more useful for assigning higher frequency spectra across the entire visible range where many lines remain unassigned.

Acknowledgments

We thank Jim Brault and Roland Schermaul for helpful conversations during the course of this work. This work has been supported by the UK Research Councils NERC and EPSRC, The Royal Society, the INTAS foundation, and the Russian Fund for Fundamental Studies.

References

[1] J.-P. Chevilliard, J.-Y. Mandin, J.-M. Flaud, C. Camy-Peyret, Can. J. Phys. 67 (1989) 1065–1084.
[2] J.M. Flaud, C. Camy-Peyret, A. Bykov, O. Naumenko, T. Petrova, A. Scherbakov, L. Sinitsa, J. Mol. Spectrosc. 183 (1997) 300–309.
[3] L.R. Brown, R.A. Toth, M. Dulick, J. Mol. Spectrosc. 212 (2002) 57–82.
[4] J.-P. Chevilliard, J.-Y. Mandin, J.-M. Flaud, C. Camy-Peyret, Can. J. Phys. 65 (1987) 777–789.
[5] C. Camy-Peyret, J.-M. Flaud, J.-Y. Mandin, A. Bykov, O. Naumenko, L. Sinitsa, B. Voronin, J. Quant. Spectrosc. Radiat. Transfer 61 (1999) 795–812.
[6] L.S. Rothman, HITRAN, 2000. Available from www.hitran.com.
[7] R. Schermaul, J.W. Brault, A.A.D. Canas, R.C.M. Learner, O.L. Polyansky, N.F. Zobov, D. Belmiloud, J. Tennyson, J. Mol. Spectrosc. 211 (2002) 169–178.
[8] P.-F. Coheur, S. Fally, M. Carleer, C. Clerbaux, R. Colin, A. Jenouvrier, M.-F. Mérienne, C. Hermanns, A.C. Vandaele, J. Quant. Spectrosc. Radiat. Transfer 74 (2002) 493–510.
[9] R.N. Tolchenov, J. Tennyson, J.W. Brault, A.A.D. Canas, R. Schermaul, J. Mol. Spectrosc. 215 (2002) 269–274.
[10] W. Zhong, J.D. Haigh, D. Belmiloud, R. Schermaul, J. Tennyson, Quart. J. Royal Meteorol. Soc. 127 (2001) 1615–1626.
[11] W. Zhong, J.D. Haigh, D. Belmiloud, R. Schermaul, J. Tennyson, Quart. J. Royal Meteorol. Soc. 128 (2002) 1387–1388.
[12] S.V. Shirin, O.L. Polyansky, N.F. Zobov, P. Barletta, J. Tennyson, J. Chem. Phys. 118 (2003) 2124–2129.
[13] R.N. Tolchenov, Program GOBLIN (to be published).
[14] R. Schermaul, R.C.M. Learner, D.A. Newnham, R.G. Williams, J. Ballard, N.F. Zobov, D. Belmiloud, J. Tennyson, J. Mol. Spectrosc. 208 (2001) 32–42.
[15] R. Schermaul, R.C.M. Learner, D.A. Newnham, J. Ballard, N.F. Zobov, D. Belmiloud, J. Tennyson, J. Mol. Spectrosc. 208 (2001) 43–50.
[16] J. Tennyson, J.R. Henderson, N.G. Fulton, Comput. Phys. Commun. 86 (1995) 175–198.
[17] J. Tennyson, B.T. Sutcliffe, J. Chem. Phys. 77 (1982) 4061–4072.
[18] J. Tennyson, B.T. Sutcliffe, Mol. Phys. 58 (1986) 1067–1085.
[19] N.F. Zobov, O.L. Polyansky, V.A. Savin, S.V. Shirin, Atmos. Oceanic Opt. 13 (2000) 1024–1028.
[20] H. Partridge, D.W. Schwenke, J. Chem. Phys. 106 (1997) 4618.
[21] O.L. Polyansky, N.F. Zobov, S. Viti, J. Tennyson, P.F. Bernath, L. Wallace, J. Mol. Spectrosc. 186 (1997) 422–447.
[22] O.L. Polyansky, N.F. Zobov, S. Viti, J. Tennyson, J. Mol. Spectrosc. 189 (1998) 291–300.

[23] M. Carleer, A. Jenouvrier, A.-C. Vandaele, P.F. Bernath, M.F. Marienne, R. Colin, N.F. Zobov, O.L. Polyansky, J. Tennyson, V.A. Savin, J. Chem. Phys. 111 (1999) 2444–2450.
[24] N.F. Zobov, D. Belmiloud, O.L. Polyansky, J. Tennyson, S.V. Shirin, M. Carleer, A. Jenouvrier, A.-C. Vandaele, P.F. Bernath, M.F. Marienne, R. Colin, J. Chem. Phys. 113 (2000) 1546–1552.
[25] H. Naus, W. Ubachs, P.F. Levert, O.L. Polyansky, N.F. Zobov, J. Tennyson, J. Mol. Spectrosc. 205 (2001) 117–121.
[26] J. Tennyson, N.F. Zobov, R. Williamson, O.L. Polyansky, P.F. Bernath, J. Phys. Chem. Ref. Data 30 (2001) 735–831.